Supplementary Materials

Electrocatalytic CO reduction to multi-carbon alcohols on functional ionic liquid-incorporated Cu-based electrodes

Jiaran Li[1,#], Lingzhi Ding[1,#], Yushan Ma[2,#], Rongxing Qiu[3], Jinlong Wan[1], Xincun Tang[2], Haikun Xu[4], Shuliang Yang[1,*], Jun Li[1,*], Li Peng[1,*]

[1]Department of Chemical and Biochemical Engineering, State Key Laboratory of Physical Chemistry of Solid Surface, College of Chemistry and Chemical Engineering, College of Energy, Xiamen University, Xiamen 361005, Fujian, China.
[2]College of Chemistry and Chemical Engineering, Central South University, Changsha 410083, Hunan, China.
[3]School of Optical and Electronic Information, Huazhong University of Science and Technology, Wuhan 430074, Hubei, China.
[4]Information and Network Center, Central South University, Changsha 410083, Hunan, China.
[#]These authors contributed equally.

[*]**Correspondence to:** Prof. Li Peng, Prof. Shuliang Yang, Prof. Jun Li, Department of Chemical and Biochemical Engineering, State Key Laboratory of Physical Chemistry of Solid Surface, College of Chemistry and Chemical Engineering, College of Energy, Xiamen University, Xiamen 361005, Fujian, China. E-mail: li.peng@xmu.edu.cn; ysl@xmu.edu.cn; junnyxm@xmu.edu.cn

EXPERIMENTAL

Materials and chemicals

Cupric acetate monohydrate ($(CH_3COO)_2Cu·H_2O$, AR), potassium hydroxide (KOH, AR), sodium perchlorate monohydrate ($NaClO_4$, AR), dimethyl sulfoxide (DMSO, AR), anhydrous ethanol (AR), isopropanol (AR) and glycol (AR) were produced by Sinopharm Chemical Reagent Co., Ltd. Deuteroxide (D_2O, 99.8 atom% D) and 1-octyl-3-methylimidazolium tetrafluoroborate ([Omim][BF_4], 99 wt%) were provided by Energy Chemical. Nafion solution (5 wt% in water and isopropanol) was obtained from Meryer (Shanghai) Chemical Technology Co., Ltd. Gas diffusion layer (YLS-30T) was purchased from Suzhou Sinero Technology Co., Ltd. CO (99.999%) was provided by Fuzhou Xinhang Industrial Gases Co., Ltd. Deionized water was used in all experiments.

Synthesis of Cu-based catalysts

The Cu-based catalysts were synthesized by a solvothermal method. Typically, $(CH_3COO)_2Cu·H_2O$ (0.002 mol) was added into a solution of 35 mL glycol in a flask. After constant ultrasonic treatment for 20 min, [Omim][BF_4] was added dropwise to the above solution. After constant ultrasonic treatment for 10 min, the mixture was transferred into a Teflon-lined stainless-steel autoclave (100 mL) for solvothermal treatment at 190 °C for 6 h, and subsequently centrifuged three times with ethanol. The sample was finally dried in vacuum at room temperature for 12 h. The content of [Omim][BF_4] was controlled to 0, 0.004, 0.008 and 0.01 mol to prepare Cu, Cu_2O-IL, Cu_2O/CuO-IL and CuO-IL, respectively.

Preparation of working electrodes

To prepare the gas diffusion electrode, 10 mg Cu-based catalyst and 20 μL Nafion solution were dispersed in 2 mL isopropanol, followed by sonication for 30 min to obtain a uniformly dispersed ink. Then 600 μL ink was dropped on a gas diffusion layer and the loading of catalyst was about 1 $mg·cm^{-2}$. The electrode was dried in a vacuum oven at 60 °C for 12 h.

Material characterizations

Powder X-ray diffraction (PXRD) patterns were collected using a Rigaku IV equipped with a Cu Kα radiation at a scan rate of 10° min^{-1}. Fourier Transform infrared spectroscopy (FT-IR) was conducted by using a Bruker Vertex 70V spectrometer. X-ray photoelectron spectroscopy (XPS) spectra were collected by a PHI Quantum 2000. Thermal gravimetric analysis (TGA) was conducted by a NETZSCH STA449F5. The morphologies of the obtained materials were characterized by scanning electron microscope (SEM, ZEISS Sigma), transmission electron microscope (TEM, Tecnai F30) and high-resolution transmission electron microscope (HRTEM, JEOL JEM-F200). ^{1}H NMR spectra were operated using a Bruker AVANCE III 500 MHz nuclear magnetic resonance spectrometer. Gas chromatography (GC) analysis was carried out on a FuLi instrument GC9790II. In-situ Raman spectra were collected at different potentials on a Raman spectrometer (XploRA Plus instrument) using a 785 nm excitation laser.

Electrocatalytic analysis

Electrochemical tests: The CORR performance was carried out in a three-electrode flow cell connected to an electrochemical workstation (CHI 660E) with 1 M KOH as electrolyte. The gas diffusion layer (1×3 cm^2) coated with catalyst was used as gas diffusion electrode. The as-prepared electrode, Hg/HgO (saturated 1 M KOH aqueous solution) and Ni foam (2×3 cm^2) were used as the working electrode, reference electrode and counter electrode, respectively. 50 mL of 1.0 M KOH solution was used as the electrolyte at both cathode and anode sides. The flow rate of cathode peristaltic pump and anode peristaltic pump were adjusted to be 20 $mL \cdot min^{-1}$, and the flow rate of CO was controlled at 20 sccm by gas flow meter.

Product analysis

To quantify the gas products during electrolysis, CO gas was delivered into the cathodic compartment at a rate of 20.0 standard cubic centimeters per minute (sccm, monitored by Sevenstar mass flow controller) and vented into a GC (FULI INSTRUMENTS, F80) equipped with a combination of 10% OV-1, Porapak N, and TDX-01 columns. A thermal conductivity detector (TCD) was mainly used to quantify H_2 concentration, and a flame ionization detector (FID) with a methanizer was used to quantitative analysis hydrocarbon species. After CORR testing, the remaining CO and gas products were decompressed into gas bags and then the controlled amount of gas

products were injected to GC by gas phase injection needle. The liquid products were detected by the ^{1}H NMR spectroscopy (Bruker AVANCE AV III 500), where DMSO was used as the reference standard, D_2O and H_2O were used as the lock solvent. The Faradaic efficiency (FE) of products was calculated as

$$FE = \frac{n \times F \times C_x \times V}{Q} \times 100\%$$

where n is the number of electrons transferred for each mole of the resulting product, C_x is the concentration of liquid products formed after electrolysis, F is the Faraday constant (96485 C mol^{-1}), V is the volume of the catholyte, and Q is the amount of charge passed through the working electrode.

Potential vs. Hg/HgO reference electrode were converted to a reversible hydrogen electrode (vs. RHE) with the Nernst equation

$$E\ (\text{V vs. RHE}) = E\ (\text{V vs. Hg/HgO}) + 0.098\ \text{V} + pH \times 0.0591$$

All the electrocatalytic reactions were carried out at ambient pressure and room temperature.

In situ Raman spectroscopy experiment

In situ Raman measurements were carried out with a XploRA Plus instrument using a 638 nm excitation laser and signals were recorded using 60 s integration in a customed-made high pressure *in situ* Raman cell setup with a three-electrode. The catalyst on glassy carbon, Pt mesh and Hg/HgO (1 M KOH) were used as the work electrode, the counter electrode and the reference electrode, respectively. The laser power was 10 mW, and the objective (Olympus, ×50) was used. Before collecting the spectra, all electrodes were electrochemically reduced by LSV. The CORR test was performed at the various potentials and the Raman signals were collected synchronously.

DFT calculations

Density functional theory (DFT) calculations were performed using the Vienna Ab-initio Simulation Package (VASP) and the projector augmented wave (PAW) method.[1,2] The Perdew-Burke-Ernzerhof (PBE) exchange-correlation functional was employed.[3] The kinetic energy cutoff was set to 400 eV. During structure optimization, sufficient spatial relaxation was performed to ensure that the maximum residual force was less than 0.03 eV Å^{-1} and the energy change was less than 1×10^{-5} eV.

A 2×2×1 supercell model was constructed using the Cu(111) plane with a vacuum layer of 20 Å. A 2×2×1 gamma k-point grid was generated using the Monkhorst-Pack method. Spin polarization and charge correction were used to perform the calculations. The Gibbs free energies (G) at 298.15 K and 1 atm were calculated as

$$\Delta G = \Delta E + \Delta ZPE - T\Delta S$$

where *ZPE* is the zero-point vibrational energy calculated using the harmonic approximation. *E* is the total energy acquired from the DFT calculation. *T* is the kelvin temperature and *S* is the entropy.

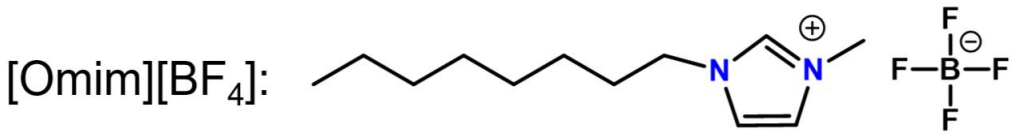

Supplementary Figure 1. Chemical structure of the ionic liquid [Omim][BF_4].

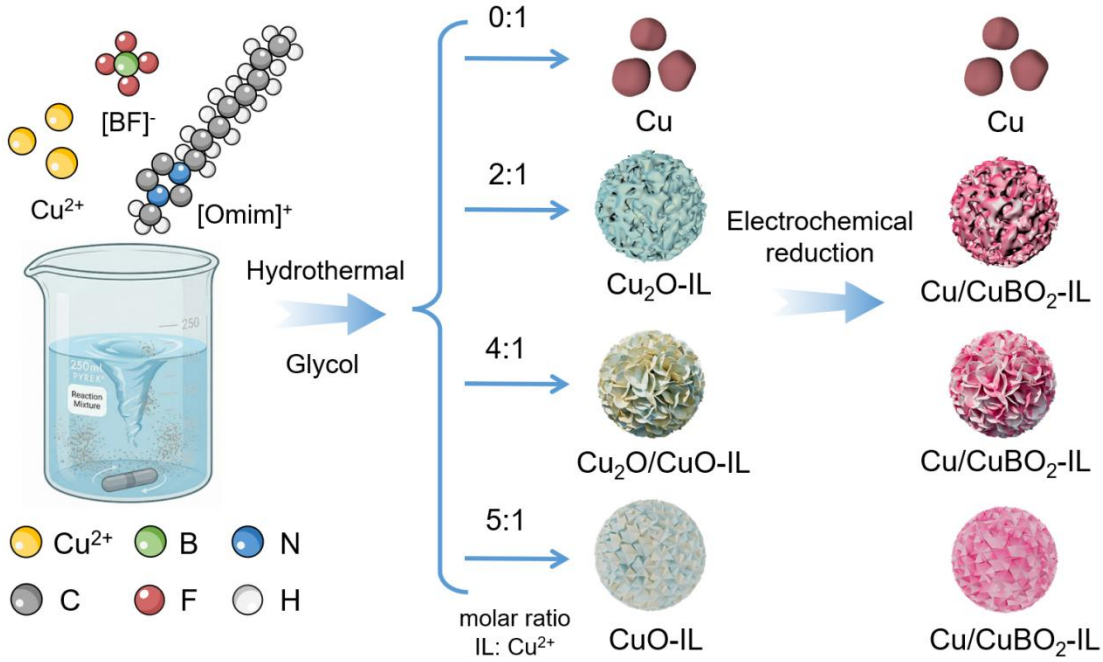

Supplementary Figure 2. Schematic illustration of the synthetic method of Cu-based catalysts with and without IL-[Omim][BF_4] modification.

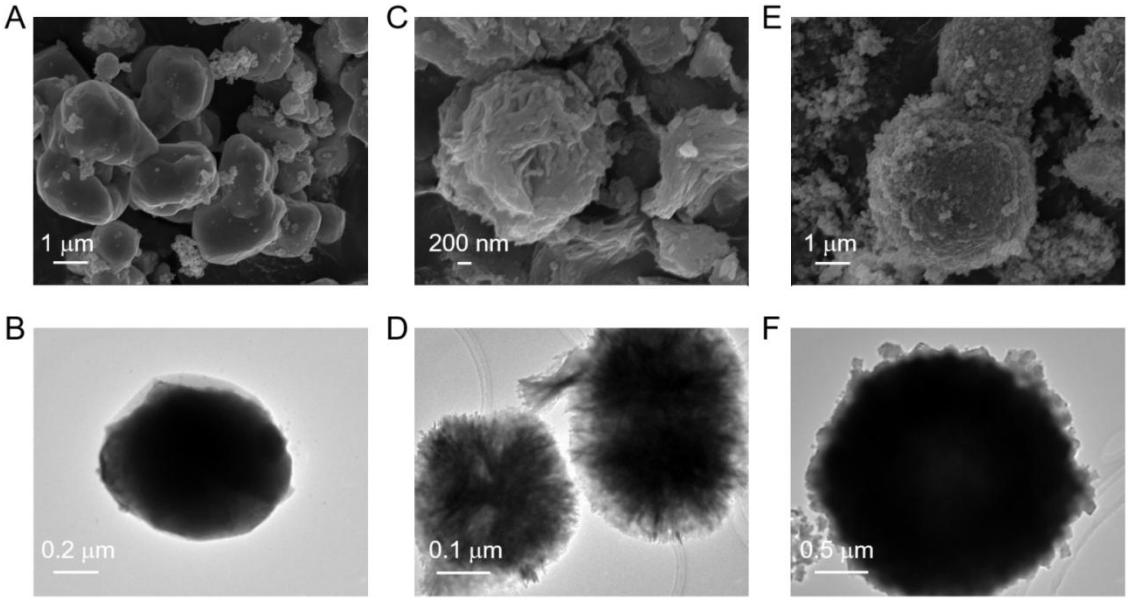

Supplementary Figure 3. SEM and TEM images of Cu (A-B), Cu_2O-IL (C-D), and CuO-IL (E-F), respectively.

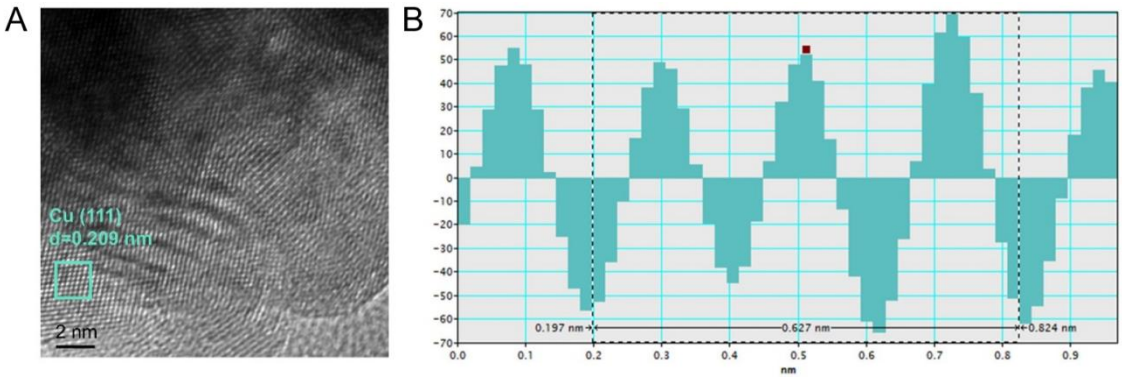

Supplementary Figure 4. HRTEM characterization of Cu. HRTEM image (A) and the corresponding intensity profile (B) measured from the region marked in image (A).

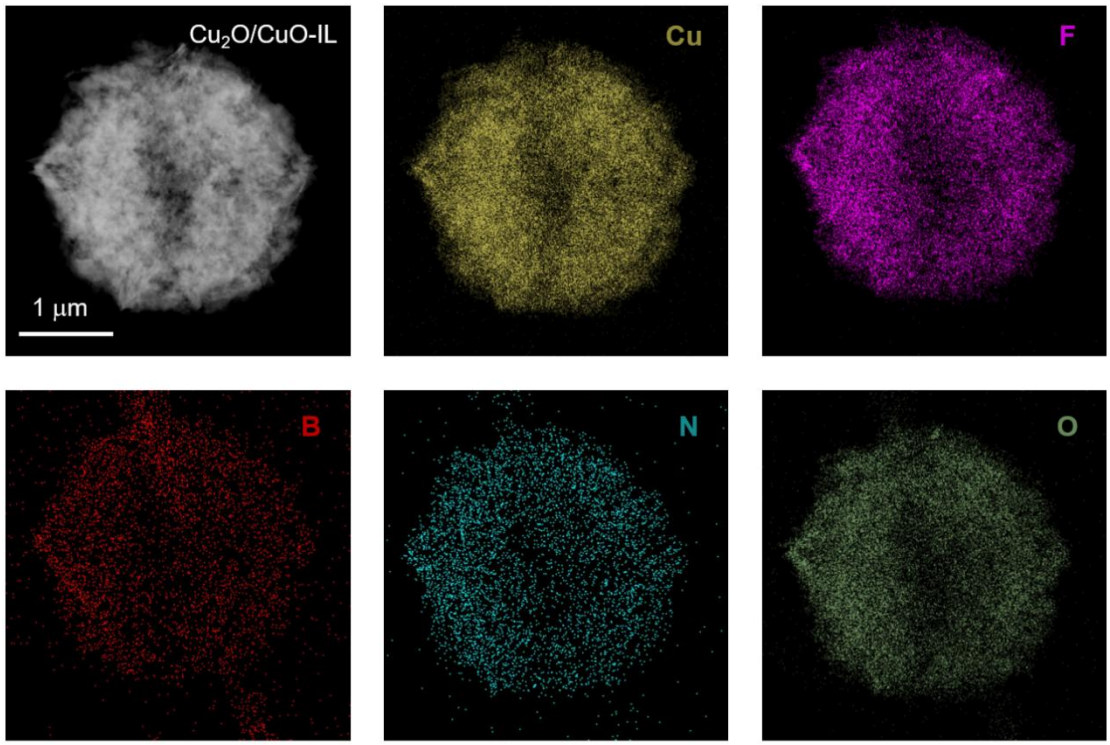

Supplementary Figure 5. HAADF-STEM and the corresponding EDX elemental mapping images of Cu_2O/CuO-IL catalyst.

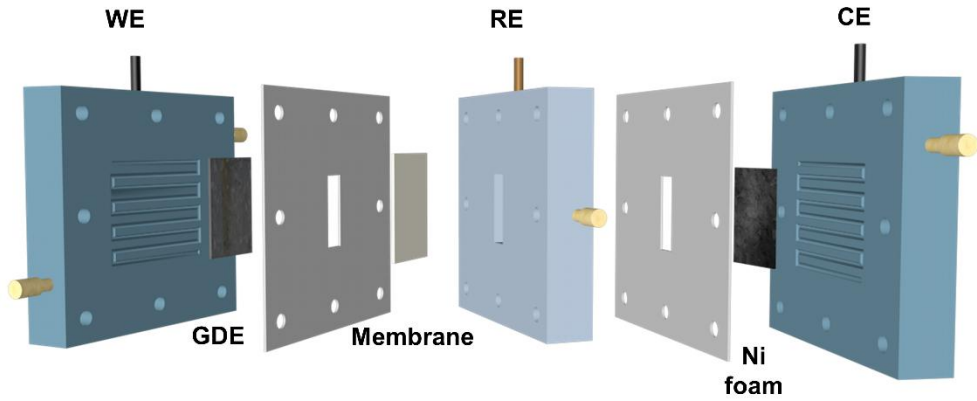

Supplementary Figure 6. Schematic diagram of the flow cell for electrocatalytic CORR.

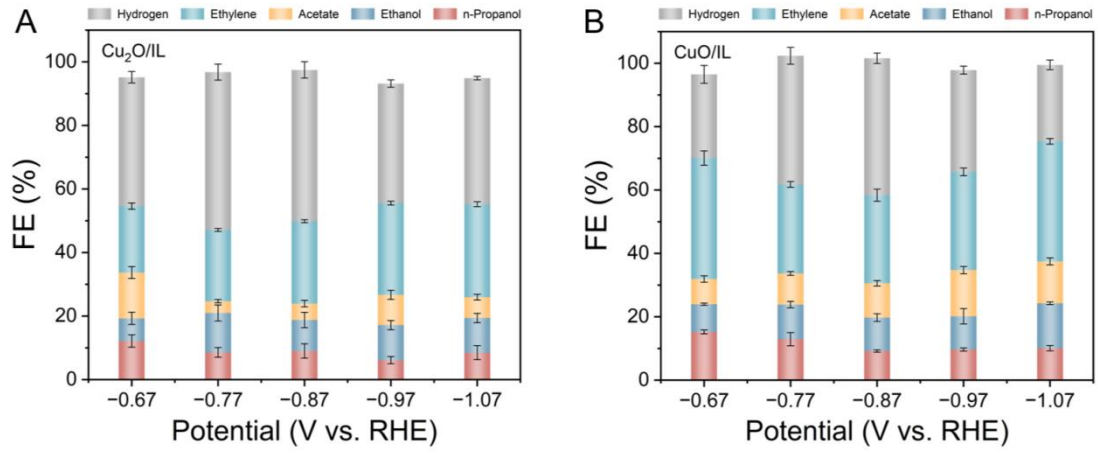

Supplementary Figure 7. FEs of products at various applied potentials for Cu_2O-IL (A) and CuO-IL (B), respectively [Error bars represent SD from three independent replicates (n = 3 per group)].

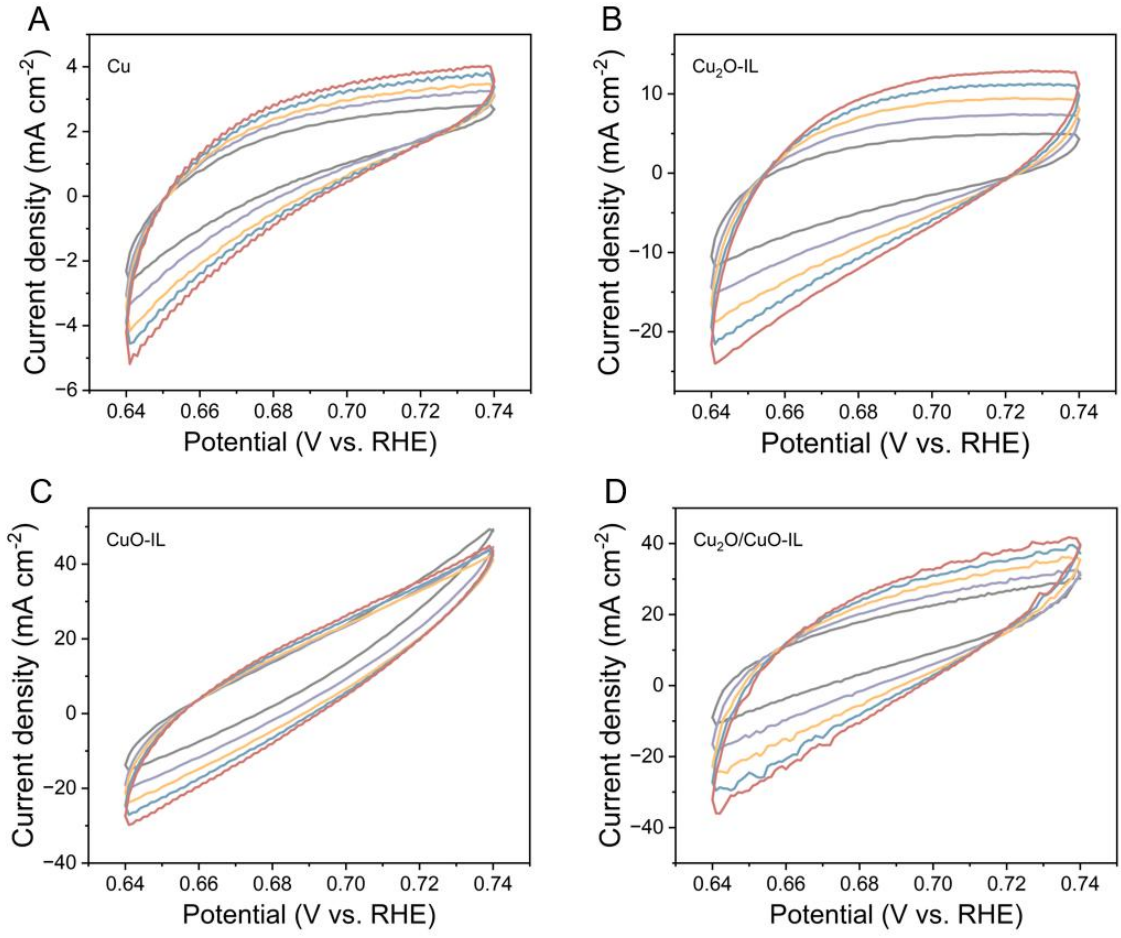

Supplementary Figure 8. CV curves of Cu (A), Cu_2O-IL (B), Cu_2O/CuO-IL (C), and CuO-IL (D) at different scan rates.

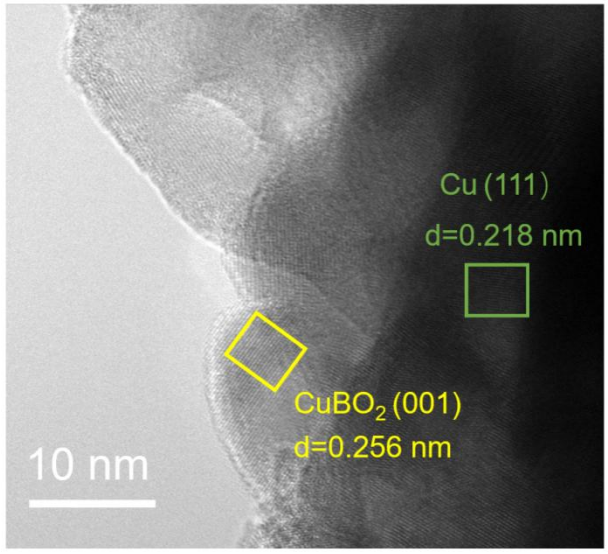

Supplementary Figure 9. HRTEM image of Cu_2O/CuO-IL catalyst after CORR.

The HRTEM image exhibited lattice spacings of 0.218 and 0.256 nm, corresponding to the Cu(111) and $CuBO_2$(001) crystal planes, respectively.

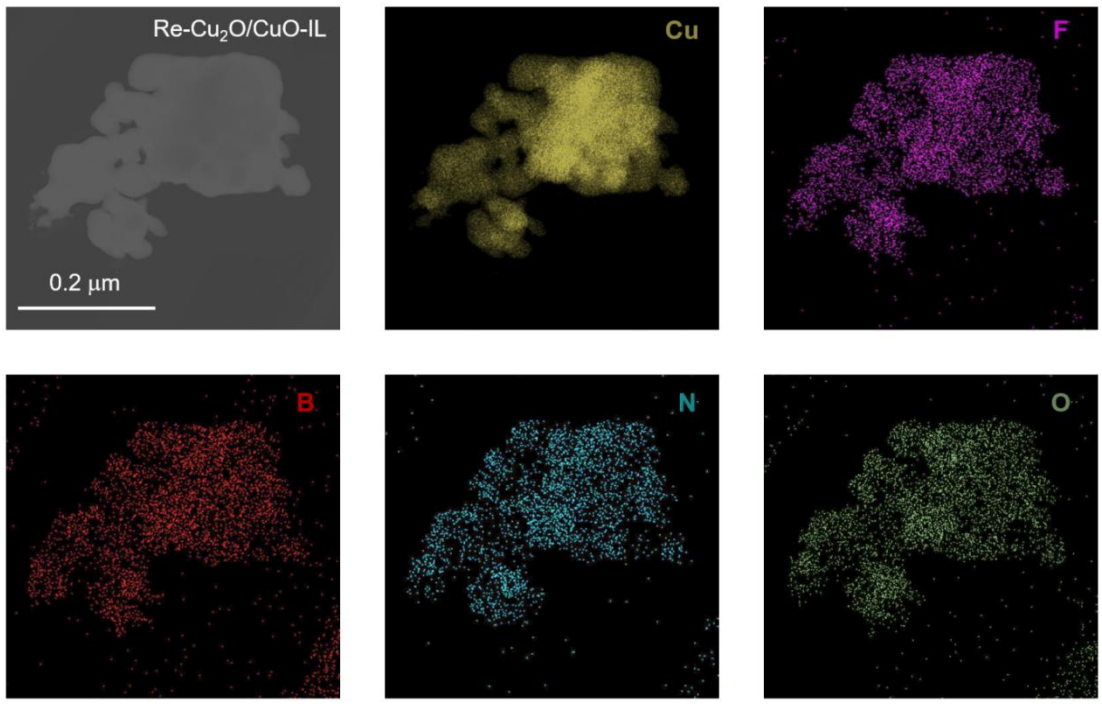

Supplementary Figure 10. TEM-EDX elemental mapping images of Cu_2O/CuO-IL catalyst after CORR.

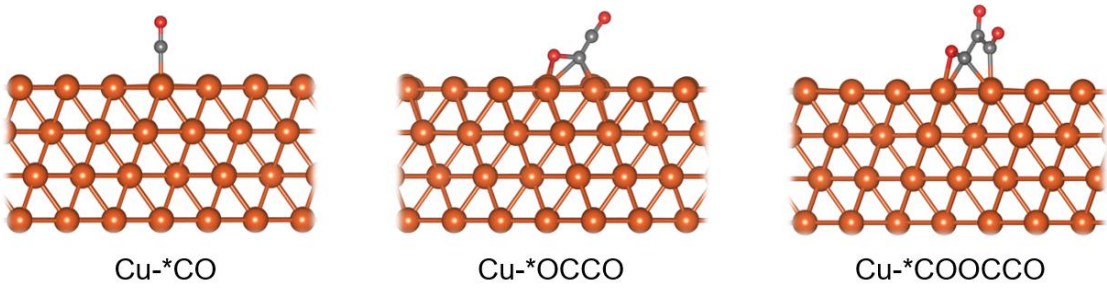

Supplementary Figure 11. Optimized adsorption configurations of reaction intermediates on Cu(111) during CORR.

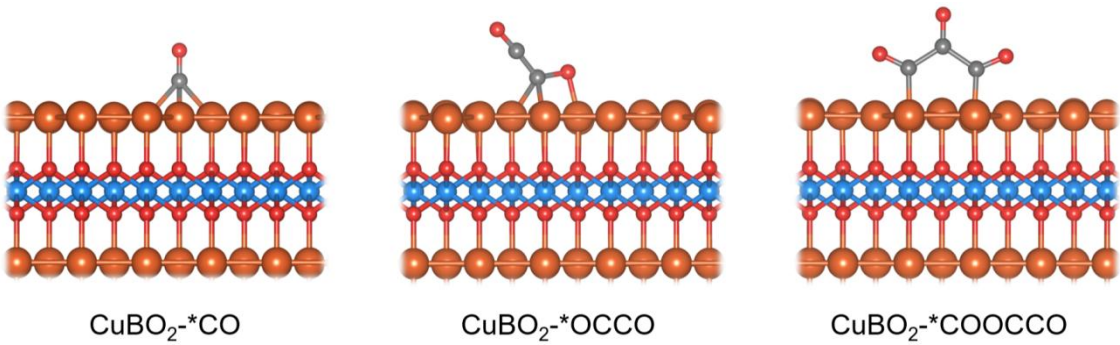

Supplementary Figure 12. Optimized adsorption configurations of reaction intermediates on $CuBO_2$(001) during CORR.

Supplementary Table 1. IL-[Omim][BF_4] content in Cu-based catalysts

Entry	Catalysts	[Omim][BF_4] content (wt%)
1	Cu_2O-IL	4.4
2	Cu_2O/CuO-IL	18.0
3	CuO-IL	23.5

Supplementary Table 2. Summary of CORR to C_{2+} alcohols performance on Cu-based electrodes

Catalysts	Potential (V vs. RHE)	$FE_{C2+\ alcohols}$ (%)	$FE_{n\text{-}propanol}$ (%)	Ref.
Cu_2O/CuO-IL	***-0.66***	***52***	***27***	***This work***
Cu/5Zn	n.r.	50	18	[4]
Ru-Cu NWs	-0.5	62	36	[5]
LSN-Cu	-0.53	73	54	[6]
Pb-Cu	-0.68	67	47	[7]
R-Cu/Au	-0.58	65	46	[8]
$CuAg_{5\%}N_{20h}$	-0.8	65	45	[9]
Cu/Cu_2O	-0.7	68	n. r.	[10]
OD-Cu	-0.42	43	26	[11]
Ag-Ru-Cu NPs	-2.75	55	36	[12]
Commercial Cu	-4	25	20	[13]
Ag-Cu NPs	-0.36	40	33	[14]
Cu ad-particles	-0.47	40	23	[15]
Fragmented Cu	-0.45	39	20	[16]
Cu plates	-0.59	27	5	[17]

REFERENCES

1. Kresse, G.; Furthmuller, J. Efficient iterative schemes for ab initio total-energy calculations using a plane-wave basis set. *Phys. Rev. B* **1996**, *54*, 11169-11186, DOI: 10.1103/PhysRevB.54.11169.
2. Kresse, G.; Joubert, D. From ultrasoft pseudopotentials to the projector augmented-wave method. *Phys. Rev. B* **1999**, *59*, 1758-1775, DOI: 10.1103/PhysRevB.59.1758.
3. Perdew, J.P.; Burke, K.; Ernzerhof, M. Generalized gradient approximation made simple. *Phys. Rev. Lett.* **1996**, *77*, 3865-3868, DOI: 10.1103/PhysRevLett.77.3865.
4. Wu, Z.; Meng, N.; Yang, R. Boosting C_{2+} alcohols selectivity and activity in high-current CO electroreduction using synergistic Cu/Zn co-catalysts. *Angew. Chem. Int. Ed.* **2024**, *64*, e202420283, DOI: 10.1002/anie.202420283.
5. Zhou, G.; Li, B.; Cheng, G. Concentrated C_{2+} alcohol production enabled by post-intermediate modulation and augmented CO adsorption in CO electrolysis. *J. Am. Chem. Soc.* **2024**, *146*, 31788-31798, DOI: 10.1021/jacs.4c10629.
6. Niu, W.; Feng, J.; Chen, J. High-efficiency C_3 electrosynthesis on a lattice-strain-stabilized nitrogen-doped Cu surface. *Nat. Commun.* **2024**, *15*, 7070, DOI: 10.1038/s41467-024-51478-4.
7. Niu, W.; Chen, Z.; Guo, W. Pb-rich Cu grain boundary sites for selective CO-to-n-propanol electroconversion. *Nat. Commun.* **2023**, *14*, 4882, DOI: 10.1038/s41467-023-40689-w.
8. Long, C.; Wan, K.; Chen, Y. Steering the reconstruction of oxide-derived Cu by secondary metal for electrosynthesis of n-propanol from CO. *J. Am. Chem. Soc.* **2024**, *146*, 4632-4641, DOI: 10.1021/jacs.3c11359.
9. Phong Duong, H.; Louis, J.; Zanna, S. Silver and copper nitride cooperate for CO electroreduction to propanol. *Angew. Chem. Int. Ed.* **2023**, *62*, e202310788, DOI: 10.1002/anie.202310788.
10. Ma, G.; Syzgantseva, O.A.; Huang, Y.; Stoian, D. A hydrophobic Cu/Cu_2O sheet catalyst for selective electroreduction of CO to ethanol. *Nat. Commun.* **2023**, *14*, 501, DOI: 10.1038/s41467-023-36261-1.

11. Jouny, M.; Luc, W.; Jiao, F. High-rate electroreduction of carbon monoxide to multi-carbon products. *Nat. Catal.* **2018**, *1*, 748-755, DOI: 10.1038/s41929-018-0133-2.
12. Wang, X.; Ou, P.; Ozden, A. Efficient electrosynthesis of n-propanol from carbon monoxide using a Ag-Ru-Cu catalyst. *Nat. Energy* **2022**, *7*, 170-176, DOI: 10.1038/s41560-021-00967-7.
13. Guo, S.; Liu, Y.; Huang, Y. Promoting electrolysis of carbon monoxide toward acetate and n-propanol in flow electrolyzer. *ACS Energy Lett.* **2023**, *8*, 935-942, DOI: 10.1021/acsenergylett.2c02502.
14. Wang, X.; Wang, Z.; Zhuang, T.-T. Efficient upgrading of CO to C_3 fuel using asymmetric C-C coupling active sites. *Nat. Commun.* **2019**, *10*, 5186, DOI: 10.1038/s41467-019-13190-6.
15. Li, J.; Che, F.; Pang, Y. Copper adparticle enabled selective electrosynthesis of n-propanol. *Nat. Commun.* **2018**, *9*, 4614, DOI: 10.1038/s41467-018-07032-0.
16. Pang, Y.; Li, J.; Wang, Z. Efficient electrocatalytic conversion of carbon monoxide to propanol using fragmented copper. *Nat. Catal.* **2019**, *2*, 251-258, DOI: 10.1038/s41929-019-0225-7.
17. Xia, R.; Lv, J.-J.; Ma, X. Enhanced multi-carbon selectivity via CO electroreduction approach. *J. Catal.* **2021**, *398*, 185-191, DOI: 10.1016/j.jcat.2021.03.034.